Electronic Supplementary Material (ESI) for RSC Advances.

Supporting Information

Continuous synthesis of $CuInS_2$ quantum dots

Tugce Akdas[1,§], Michael Haderlein[1], Johannes Walter[1], Benjamin Apeleo Zubiri[2], Erdmann Spiecker[2], Wolfgang Peukert[1]

[1] Institute of Particle Technology (LFG), Friedrich-Alexander-Universität Erlangen-Nürnberg (FAU), Cauerstr. 4, 91058 Erlangen, Germany

[2] Center for Nanoanalysis and Electron Microscopy (CENEM), Friedrich-Alexander-Universität Erlangen-Nürnberg (FAU), Cauerstr. 6, 91058 Erlangen, Germany

[§] present address: CEA Grenoble, INAC, SyMMES, STEP, 17 rue des Martyrs, 38054 Grenoble, France

1. *Theoretical Comparison of the Reactors*

Synthesis of $CuInS_2$ QDs was performed in two continuous-flow reactors, namely in a tubular reactor (TR) and in a microreactor (MR) and additionally in batch operation mode in a three-neck round-bottom flask. Simplified flowsheets of the two flow reactors are shown in Figure S1. The precursor solution was pumped into the flow reactors with syringe pumps using varying flow rates resulting in residence times $\bar{\tau}$ ranging from approximately 1.5 min to 26 min in the performed experiments. For details see Experimental Part (section 6).

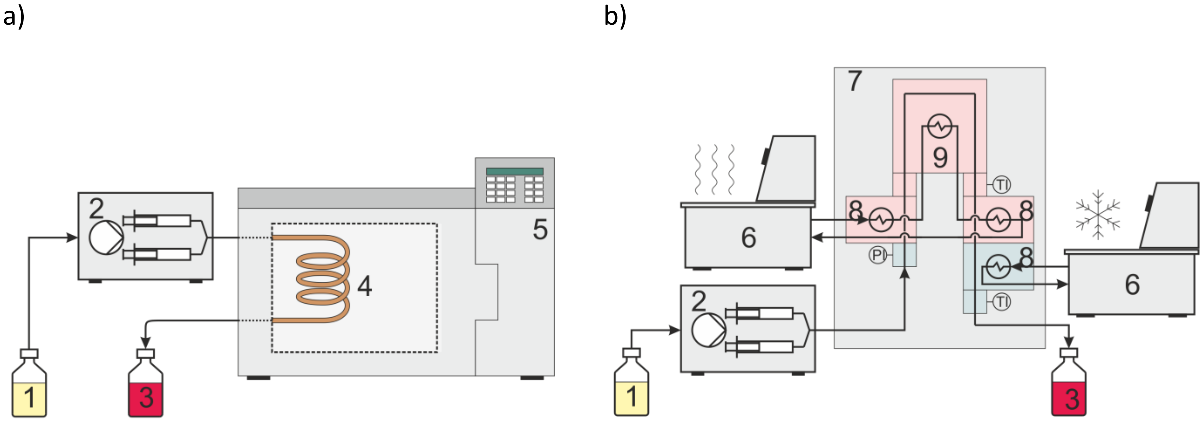

Figure S1: Sketch of a) the self-constructed tubular reactor TR and the b) microreaction system MR: In both cases, the feed (1) is introduced into the reactor setup by a syringe pump (2) and the product is collected at the outlet (3). In case of the TR, the reaction is run in a stainless steel capillary (4) which is placed in an oven (5) with internal temperature control. In case of the MR, two thermostats (6) are heating and cooling, respectively, several heat exchangers (8) to ensure accurate temperature control of the setup. The main reaction zone is the meander reactor (9). The MR elements are mounted on a base plate (7).

The two flow reactors and the batch reactor were characterized with regard to mixing and heat transfer to allow for comparison and evaluation of the processes. Most of the equations used in the following can be found in textbooks[1-6], additional literature is provided where necessary.

The Prandtl number Pr is a measure for the ratio between momentum and heat transfer within a fluid and is given by

$$Pr = \frac{\eta \cdot c_p}{\lambda} = \frac{\nu}{a} \qquad (1)$$

where η is the dynamic viscosity of the fluid, c_p is its specific heat capacity, λ the thermal conductivity, ν is its kinematic viscosity and a is the fluids' conductibility of temperature. It was assumed that the impact of the reactants on the physical parameters of the solvent 1-ODE is negligible. The parameters used for 1-ODE[7] are $\eta = 0.000313\,Pa \cdot s$, $c_p = 2781\,J/(kg \cdot K)$, $\lambda = 0.0763\,W/mK$ and $\nu = 3.97566 \cdot 10^{-7}\,m^2/s$ at $503.15\,K$ resulting in $\mathrm{Pr} \sim 11$.

The dimensionless Reynolds number Re is defined as the ratio of the inertia force F_ρ and the frictional force F_η. In stirred tank reactors, the Re number is calculated as

$$Re = \frac{F_\rho}{F_\eta} = \frac{f \cdot d_{h,st}^2}{\nu} \tag{2}$$

where f gives the number of rotations of the stirrer ($f = 16.7\,s^{-1}$) and $d_{h,st}$ is the hydraulic diameter of the magnetic stir bar ($d_{h,st} = 0.0164\,m$). To determine whether flow in a tube is laminar or turbulent, Re is calculated according to

$$Re = \frac{F_\rho}{F_\eta} = \frac{\rho \cdot L \cdot u}{\eta} = \frac{L \cdot u}{\nu} \tag{3}$$

where ρ is the density of 1-ODE ($\rho = 788.8\,kg \cdot m^{-3}$), L is the characteristic dimension of the reactor (TR: diameter $d = 2.2\,mm$ in cylindrical tube; MR – Heat Exch: piston ring with hydraulic diameter $d_h = 0.225\,mm$; MR – RTR: rectangular geometry $d_h = 2.308\,mm$), u is the velocity of the reaction solution (ranging from $2.2\,mm \cdot s^{-1}$ to $24\,mm \cdot s^{-1}$ in the present experiments). The calculated Reynolds numbers Re (TR: 20; MR: 3; batch: 11300, see Table S1) demonstrate that the flow is laminar in both flow reactors, it reveals turbulent mixing in the batch reactor.

While the temperature and heating rate for the experiments in MR and batch are known from in-situ measurements, they must be approximated for the continuous experiments in TR. The temperature evolution of the reaction solution in the pipe is obtained by an energy balance resulting in the following equation

$$\frac{T_{rs} - T_0}{T_w - T_{rs}} = \frac{\pi \cdot d \cdot h \cdot x}{\dot{m} \cdot c_p} \tag{4}$$

where T_{rs} is the temperature of the reaction solution, T_0 is the initial temperature (room temperature, $T_0 = 20$ °C), T_w is the wall temperature ($T_w = 240$ °C), d is the tube diameter, x is the position along the tube and $\dot{m}$ is the mass flow rate. The convective heat transfer coefficient h is calculated via the Nusselt number Nu according to the Manlapaz-Churchill correlation[8-9], leading to a value of $h = 120\,W\,m^2\,K^{-1}$. For reasons of completeness, the according values have also been calculated for the other reactors (see Table S1), respecting the individual geometries.

The temperature curves in Figure S2 show the comparison of the heating period for all three reactors. It becomes obvious that heat transfer is most efficient in the MR where only a few seconds are needed to reach the desired reaction temperature (240 °C). In TR, it takes ~3.5 min to reach 240 °C for all flow rates, while heating up is slowest in the batch reactor with ~13 min. This effect of the ratio of surface area of the respective reactor to volume of reaction solution that needs to be heated is therefore clearly visible by the heating rates. With a tube diameter of only 2.2 mm in the TR or 220 µm in the MR, a lower heat transfer coefficient still results in a faster heating rate.

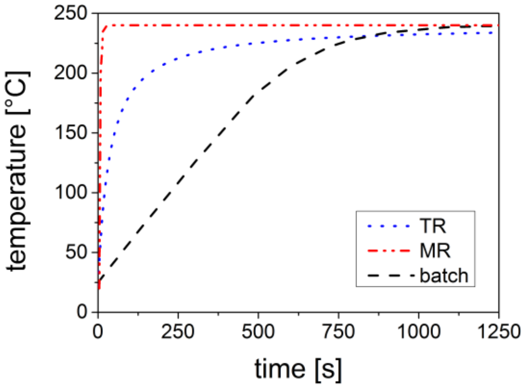

Figure S2: Comparison of temperature evolution in the three reactors, namely in the tubular reactor (TR, blue dotted line), the microreactor (MR, measured data, cyan dashed line the batch reactor) and the batch reactor (measured data, purple dashed-dotted line). The temperature profile of the batch reactor has been smoothened.

Table S1: Comparison of mixing and heating in the three reactor systems, namely the tubular reactor (TR), the microreactor (MR) and the flask (batch reactor). The two separate parts of the MR, namely the heat exchanger (MR - Heat Exch) and the residence time reactor (MR - RTR), were separately considered for the calculations.

Reactor	Re [-]	Nu [-]	h W m^{-2} K^{-1}	$\dot{Q}$ [W]
TR	20	3.8	120	5
MR – Heat Exch	13	7.5	1300	24
MR – RTR	3	3.7	28	1
Batch	11300	-	2400	9

2. *Reactions in the microreactor*

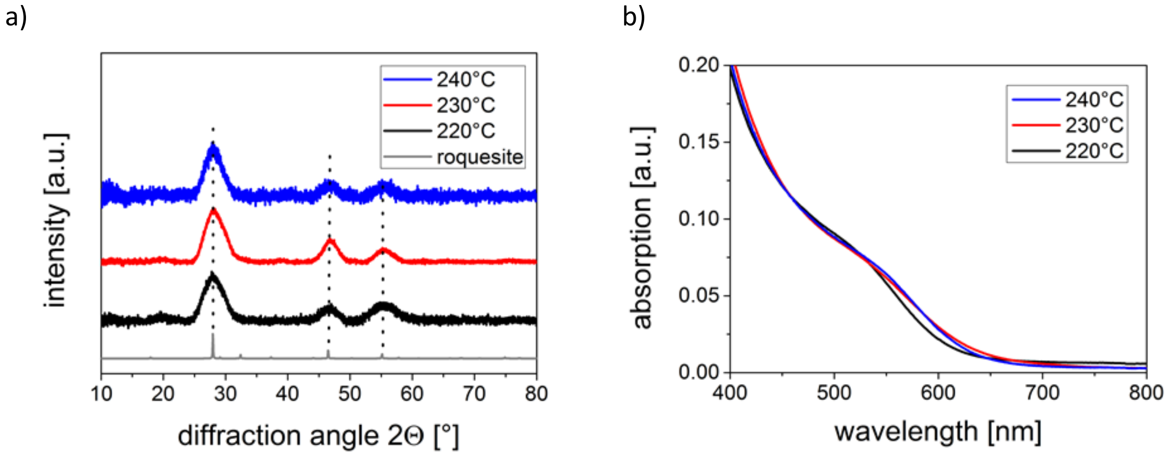

Figure S3: (a) Comparison of XRD pattern and (b) absorption spectra of $CuInS_2$ QDs synthesized at 220 °C ($\bar{\tau}$ = 10.5 min), at 230 °C ($\bar{\tau}$ = 6.8 min) and at 240 °C ($\bar{\tau}$ = 3.0 min). The precursor preparation temperature was 170 °C.

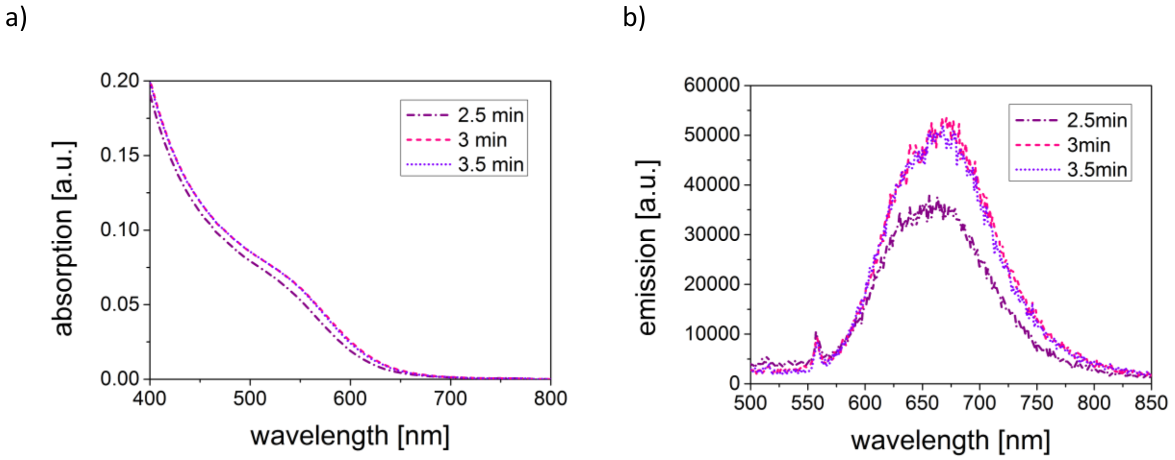

Figure S4: Absorption (a) and emission spectra (b) of samples synthesized in the MR with a reaction temperature of 240°C (precursor preparation at 170 °C).

3. Batch reactions in the flask

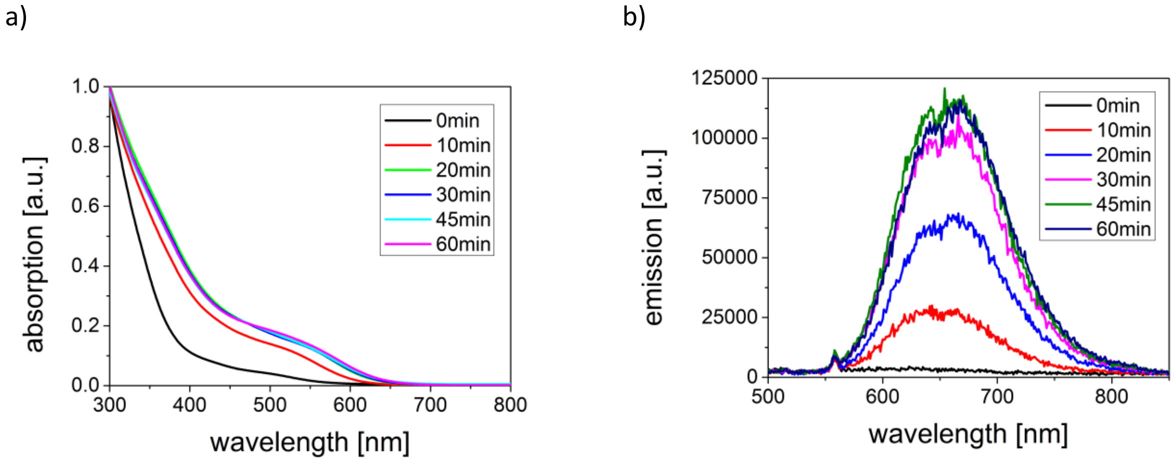

Figure S5: Absorption (a) and emission spectra (b) of samples synthesized in batch at 240 °C (precursor preparation at 170 °C).

4. *Comparison of products synthesized in various reactors*

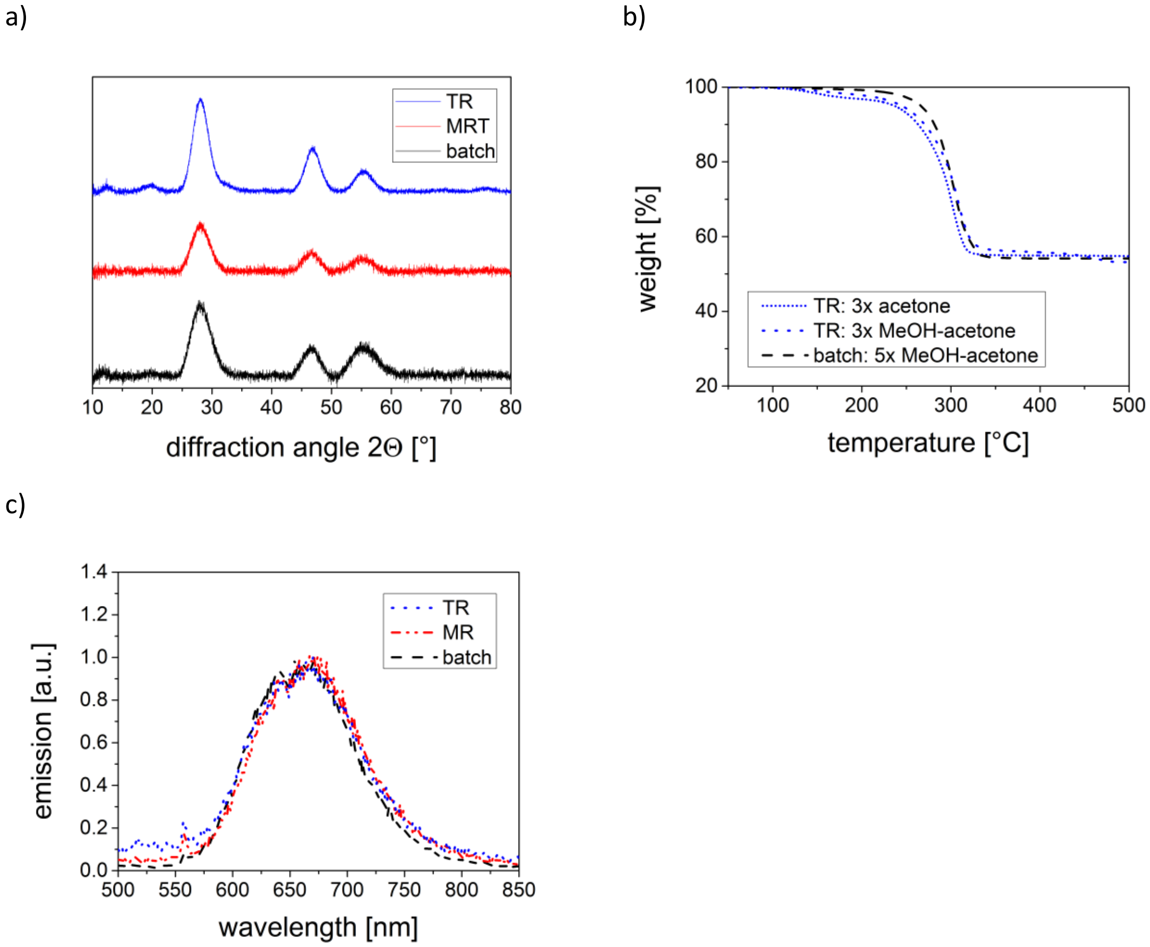

Figure S6: a) XRD of $CuInS_2$ samples synthesized at 240°C in the three different reactors TR, MR and batch. b) TGA of TR and batch samples purified with acetone or MeOH-acetone: five centrifugation cycles in case of batch synthesis and three centrifugation cycles in case of continuous-flow synthesis. c) Comparison of emission spectra of $CuInS_2$ QDs synthesized in batch and in continuous, respectively. The reaction temperature was 240 °C in all reactions; corresponding $\bar{\tau}$ were 5 min in the tubular reactor (TR), 3.0 min in the microreactor (MRT) and 45 min in the batch reactor.

5. *Summary of AUC results*

Table S2: Data derived from sedimentation velocity analytical ultracentrifugation (SV-AUC) experiments on TR and batch samples.

sample	s [sved]	D [10^{-6} cm^2 s^{-1}]	x_h [nm]	v_{bar} [cm^3 g^{-1}]	ρ [g cm^{-3}]	x_c [nm]	d_{shell} [nm]
TR - 5 min	12.03	1.79	4.42	0.678	1.475	2.41	1.00
TR - 10 min	14.86	1.73	4.58	0.639	1.565	2.61	0.99
TR - 20 min	16.04	1.73	4.58	0.616	1.623	2.68	0.95
Batch	11.81	1.74	4.54	0.698	1.433	2.42	1.06

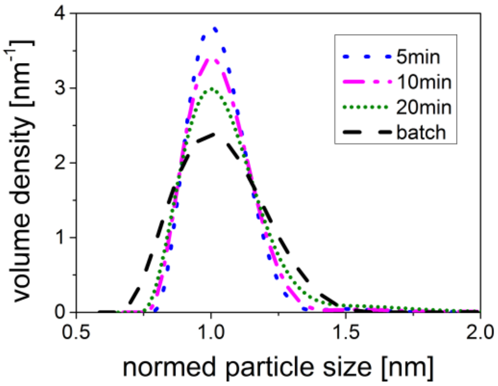

Figure S7: Normed results of SV-AUC experiments performed to compare PSDs of TR samples with the PSD of the batch product.

6. Experimental Details

Chemicals: All chemicals were used as received and without further purification. Copper(I) acetate (CuAc, 97%), indium(III) acetate (In(Ac)$_3$, 99,999%), 1-octadecene (1-ODE, 90%) and 1-dodecanethiol (1-DDT, ≥98%) were obtained from Aldrich. CuAc and In(Ac)$_3$ were stored in a nitrogen-filled glovebox to prevent degradation. Toluene (99.5%) was obtained from Acros. Acetone (≥99.8%), methanol (MeOH, ≥99.9%) and chloroform ($CHCl_3$, ≥99%) were obtained from Roth.

Tubular Reactor: A stainless steel capillary with an inner diameter of 2.2 mm was bent to a helical coil and placed in an oven with internal temperature control. The length of the capillary inside the oven was 3.4 m. A double syringe pump (Sykam S 1610) conveyed the feed via PTFE capillaries into the inlet. Mean residence times were adjusted by promoting the feed into the capillary with different velocities.

Microreaction System: A modular setup was used for the continuous synthesis (Ehrfeld Mikrotechnik BTS GmbH). It consisted of several heat exchanger units to heat and cool down the reaction solution and a meander reactor to allow for a well-defined residence time. Both, the meander reactor and the heat exchanger were powered by a Julabo HC thermostat. A double syringe pump conveyed the feed into the inlet.

Preparation of Precursor: The procedure of precursor preparation was carried out using a Schlenk line, similar to a recent report by Tian *et al*. A 250 ml round three-necked bottom flask was placed in a heating mantle. One neck was connected to a condenser and the other sealed by a septum. A thermocouple was used to provide accurate temperature control. 1-ODE was degassed minimum 30 min prior to synthesis. CuAc, In(Ac)$_3$, 1-DDT and 1-ODE were added into the flask, degassed by pulling vacuum for 10 min, followed by N_2 bubbling for one minute. This procedure was repeated three times. Afterwards, the mixture was heated to 170 °C and hold for 30 min, then cooled down to room temperature by using a water bath. Undissolved solid sedimented and was discarded.

Continuous Synthesis of CuInS$_2$ Quantum Dots: Prior to each reaction, the channels of the reactors were cleaned thoroughly by pumping different solvents, namely pure absolute ethanol first, followed by toluene and finally 1-ODE$_{\text{techn}}$. During the heating period, 1-ODE$_{\text{techn}}$ was looped through the setup. Once reaction temperature was reached, the precursor solution was pumped in with flow rates ranging from 0.5 ml min^{-1} to 7.0 ml min^{-1}. This corresponds to mean residence times $\bar{\tau}$ from ~1.5 min to ~26 min as calculated by

$$\bar{\tau} = \frac{V}{\dot{V}} = \frac{l}{\bar{v}} \tag{5}$$

where V is the volume of the reactor (TR: 12.9 ml; MR: 13.7 ml), $\dot{V}$ is the volume flow, l is the length of the tube (TR: 3.4 m; MR: 1.04 m) and $\bar{v}$ the mean flow velocity. The corresponding datasets are shown in Figure S8. The product was collected at the outlet of the reactor after the system had reached a steady state.

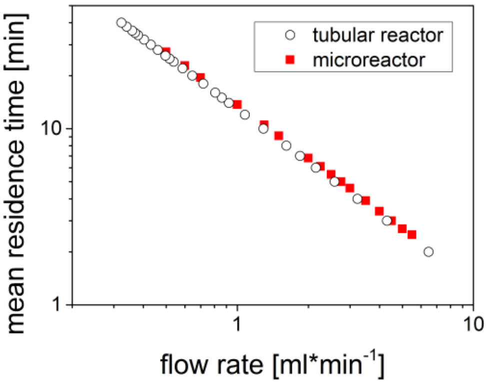

Figure S8: Mean residence times for various flow rates in the tubular reactor (black hole circles) and the microreactor (red squares). The markers indicate the process conditions tested within this work.

Batch Synthesis of CuInS$_2$ Quantum Dots: First, the precursor was prepared using a Schlenk line, as described above. For batch synthesis, the precursor solution was heated up to 240 °C and aliquots were taken to monitor growth. The reaction was stopped after 45 min by cooling down to room temperature with a water bath.

Purification: Washing of the nanocrystals was conducted by first adding one equivalent (eq.) CHCl$_3$ to the reaction solution, followed by the addition of one eq. of MeOH and three eq.s of acetone to flocculate the nanocrystals. After centrifugation for 10 min at 8000 rpm (8240 g), the supernatant was discarded and the obtained precipitate was redispersed in CHCl$_3$. This cycle was performed several times. The final product can be redispersed in any lipophilic solvent, such as toluene, hexanes or chloroform.

Materials Characterization:

TEM: High-resolution (HR) TEM, bright field (BF) TEM and scanning TEM (STEM) were performed with a double aberration-corrected FEI Titan^3 Themis 300 transmission electron microscope operated at 200 kV. All HRTEM micrographs were obtained at a reduced spherical aberration (Cs < 10 µm) and minimum contrast of the support film. BF-TEM was used to enhance the contrast between the carbon substrate and the particles. STEM imaging exhibits an enhanced mass-thickness contrast enabling an easier interpretation of the measured image intensities. The electron beam irradiation of the imaged area was minimized to avoid ripening of the nanocrystals. To prevent agglomeration, the nanocrystal dispersions in chloroform solution were put in an ultrasonic bath for 2 minutes and were then drop-cast onto TEM sample grids with ultrathin carbon films supported by a lacey carbon film (Ted Pella Inc. USA).

ICP-OES: Dried powder samples (~15 mg) were mineralized using aqua regia (4 ml) and diluted with millipore water. Analysis was performed with an ICP-OES Spectrometer Optima8300 from Perkin Elmer.

X-ray diffraction (XRD): Analysis in Bragg-Brentano geometry was performed with a Bruker AXS Advance D8 instrument using Cu K_α radiation ($\lambda_{K\alpha}$ = 1.54 Å). The XRD patterns were measured in the 2θ range between 10° and 80° with a step size of 0.02°. The diffractometer was equipped with a 1-dimensional Vantec-1 high-speed detector and a rotating sample stage. Low background sample cups with a vicinal (911) Si crystal of 25 mm diameter from Bruker AXS were used as substrates for the scans. All samples were prepared by drop-casting of the dispersion onto the substrate and evaporation of the solvent. The mean crystallite size x_c was calculated from the full width at half maximum (FWHM) of the diffraction peaks by using the Scherrer Equation assuming Gaussian shaped peaks:

$$x_c = \frac{K \cdot \lambda}{\beta \cdot \cos\theta} \tag{6}$$

where K is a dimensionless shape factor (here: 0.9), λ is the wavelength of the X-ray (λ_{K_α} = 1.54 Å), β is the line broadening at half maximum intensity and θ is the Bragg angle.

Thermogravimetric analyses (TGA): TGA were performed on a TGA Q50 from TA Instruments. Masses of ~15 mg dried powder samples were heated up to 500 °C in a platinum pan under a constant nitrogen flow of 40 ml min^{-1}, with a heating rate of 10 K min^{-1}. TA Instrument Analysis Software was used to analyse and export the data.

Optical Characterization: Absorption spectra were recorded by means of a Perkin Elmer Lambda35 two-beam spectrophotometer using a slit width of 2 nm and a scan rate of 240 nm min^{-1}. Emission spectra were collected on a Fluorolog Horiba Jobin Yvon using a slit width of 2 nm. Quartz glass cuvettes with an optical path length of 10 mm were used. The powders were redispersed in n-hexane and their optical density was set to 0.1 at a wavelength of 480 nm.

AUC: Analytical ultracentrifugation sedimentation velocity experiments (SV-AUC) were performed to determine the size and core-shell properties of the $CuInS_2$ QDs in solution. A modified preparative centrifuge, type Optima L-90K from Beckman Coulter (USA), was used to acquire SV-data.[10-11] Two-sector titanium centerpieces from Nanolytics (Germany) with an optical path length of 12 mm were used and data were acquired every 90 seconds at 25000 rpm, 25 °C and a radial resolution of 50 µm. Samples were diluted in toluene up to equal absorbance of 1.0 at 350 nm in the AUC cell. The solvent density and viscosity were measured using the densitometer DMA5000 in combination with the viscometer Lovis 2000, both from Anton Paar (Austria). Values were found to be 0.8622 g cm^{-3} and 0.552 mPas for the density and viscosity, respectively. The core density of bulk $CuInS_2$ was 4.739 g cm^{-3}. SV-multiwavelength intensity data were recorded from 300 nm to 600 nm. Intensity data at 360 nm were used for further evaluation. The sedimentation and diffusion coefficients of the QDs become accessible through Lamm's equation and are linked to the particle diameter and density through Stokes' and Einstein's laws. For determination of the structure of the $CuInS_2$ QDs we used the same procedure as presented recently by *Akdas et al.*[12] For the QDs synthesized in the continuous reactor the weight averaged sedimentation and diffusion coefficients were used. They provide more accurate information on the particulate properties than the peak maxima of the 2-dimensional distribution because the whole distribution is considered. However, for the batch synthesis the values from the peak maxima had to be used since agglomeration in the batch sample falsified the weight averaged sedimentation and diffusion coefficients and consequently the obtained parameters. Further information regarding the applied data analysis is available in literature.[13-14]

7. References

1. Lienhard, J. H. I.; Lienhard, J. H. V., A heat transfer textbook. third edition ed.; Phlogiston Press: Cambridge, Massachusetts, USA, 2008.
2. Holman, J. P., Heat Transfer. 6th edition ed.; McGraw-Hill: New York, 1986.
3. VDI, V. D. I., VDI Wärmeatlas. (GVC), V.-G. V. u. C., Ed. Springer: Heidelberg, 2005.
4. Christen, D. S., Praxiswissen der chemischen Verfahrenstechnik. Springer: 2009.
5. Baehr, H. D.; Stephan, K., Wärme- und Stoffübertragung. Springer: 2010.
6. Martin, H., *Lecture on heat transfer II* Universität Karlsruhe, TH: 1990.
7. Liessmann, G.; Schmidt, W.; Reiffarth, S. Data compilation of the saechsische olefinwerke Boehlen. Recommended thermophysical data. 1995, p. 35.
8. Manlapaz, R. L.; Churchill, S. W., Fully-developed laminar convection from a helical-coil. *Chemical Engineering Communications* **1981,** *9* (1-6), 185-200.
9. Xue, Z. L.; Terepka, A. D.; Hong, Y., Synthesis of silver nanoparticles in a continuous flow tubular microreactor. *Nano Letters* **2004,** *4* (11), 2227-2232.
10. Strauss, H. M.; Karabudak, E.; Bhattacharyya, S.; Kretzschmar, A.; Wohlleben, W.; Coelfen, H., Performance of a fast fiber based UV/Vis multiwavelength detector for the analytical ultracentrifuge. *Colloid and Polymer Science* **2008,** *286* (2), 121-128.
11. Walter, J.; Loehr, K.; Karabudak, E.; Reis, W.; Mikhael, J.; Peukert, W.; Wohlleben, W.; Coelfen, H., Multidimensional analysis of nanoparticles with highly disperse properties using multiwavelength analytical ultracentrifugation. *ACS Nano* **2014,** *8* (9), 8871-8886.
12. Akdas, T.; Walter, J.; Segets, D.; Distaso, M.; Winter, B.; Birajdar, B.; Spiecker, E.; Peukert, W., Investigation of the size-property relationship in CuInS2 quantum dots. *Nanoscale* **2015**.
13. Schuck, P., Size-distribution analysis of macromolecules by sedimentation velocity ultracentrifugation and Lamm equation modeling. *Biophysical Journal* **2000,** *78* (3), 1606-1619.
14. Brown, P. H.; Schuck, P., Macromolecular size-and-shape distributions by sedimentation velocity analytical ultracentrifugation. *Biophysical Journal* **2006,** *90* (12), 4651-4661.